Author/s:
Quigley, M;Werner, T;Tang, Y;Clark, D;Griffin, J;Yang, H

Title:
Exposure of Australian dams to seismic hazard from proximal faults

Date:
2025-06-01

Citation:
Quigley, M., Werner, T., Tang, Y., Clark, D., Griffin, J. & Yang, H. (2025). Exposure of Australian dams to seismic hazard from proximal faults. Environment Systems and Decisions, 45 (2), pp.24-. https://doi.org/10.1007/s10669-025-10015-4.

Persistent Link:
https://hdl.handle.net/11343/362152

Environment Systems and Decisions (2025) 45:24
https://doi.org/10.1007/s10669-025-10015-4

Exposure of Australian dams to seismic hazard from proximal faults

Mark Quigley[1] · Tim Werner[1] · Yuxiang Tang[1] · Dan Clark[2] · Jonathan Griffin[2] · Haibin Yang[3]

Accepted: 10 April 2025 / Published online: 21 April 2025

Abstract

The purpose of this study is to obtain estimates of ground surface rupture and ground motion hazards at standardised scales useful for general reference and regional comparisons of dams (n = 548) registered with the Australian National Committee on Large Dams (ANCOLD). Geospatial and statistical methods are used to investigate the exposure of dams to seismic hazard from 409 faults in the Geoscience Australia Neotectonic Features Database (NFD). We identify 216 faults at distances less than 100 km from 428 dams and measure 4055 fault-to-dam distances. At least 31 dams are located within 1 km of NFD fault traces and at least 16 of these dams could reside within NFD primary fault zones. Estimates of NFD maximum moment magnitudes ($M_{w,max}$) from fault area and length regressions range from $5.6 \leq M_w \leq 7.9$. Average (AD) and maximum (MD) NFD fault displacements for $M_{w,max}$ events range from 0.3 m ≤ AD ≤ 4.4 m and 0.9 m ≤ MD ≤ 8.4 m. Distance-probability regressions for distributed ground surface rupture suggest approximately 40 dams have a ≥ 10% probability of ground surface rupture occurring in the area encompassing the dam in a $M_{w,max}$ event. Peak ground accelerations (PGA) and pseudo-spectral acceleration at 1.0 s (PSA[1.0 s]) are estimated for $M_{w,max}$ at dam sites using the same set of ground motion models (GMMs) for the 2023 National Seismic Hazard Assessment (NSHA23), assuming engineering rock site conditions with a time-averaged shear wave velocity between the surface and 30 m sediment depth (VS30) of 760 m/s. Of the 4055 $M_{w,max}$ scenarios considered in total, 3579 $M_{w,max}$ scenarios produce 85th percentile PGA ≥ 0.1 g at dam sites and 2844 scenarios produce 85th percentile PSA[1.0 s] ≥ 0.1 g. Comparison with 1:5,000 annual exceedance probability (AEP) PGA and PSA[1.0 s] estimates from the NSHA23 indicate there are 404 out of 428 dams where NFD $M_{w,max}$ PGA are greater than NSHA23 values, and 422 instances where PSA[1.0] > NSHA23. Proximity to NFD faults imparts a first-order control on relative hazard. A large increase in the number of identified NFD faults over the last decade suggests further research will continue to increase NFD fault populations. NFD fault slip rates and $M_{w,max}$ are important parameters in seismic hazard analysis for many dams but exhibit large epistemic and aleatoric uncertainties. Improving the characterisation of NFD faults through acquisition of direct fault-specific seismic hazard information (e.g., single-event displacements, slip rates, inter-event times, frequency-M_w distributions, segmentation scenarios) will assist with hazard profiling for many ANCOLD dams.

Keywords Earthquakes · Seismic hazard · Dams · Fault displacement hazard

1 Introduction

The seismic design of dams in Australia is relatively young compared to countries like the U.S. or Japan, largely due to the perception that Australia is a tectonically stable region with lower seismic risks. Early dams built before the 1970s generally did not consider seismic loading in their design. However, as global understanding of seismic hazards improved, Australian engineers began integrating seismic considerations into dam design, particularly from the late twentieth century onwards. Many dams built before the 1970s were designed without specific seismic design criteria, as earthquakes were not seen as a major concern. After

✉ Mark Quigley
mark.quigley@unimelb.edu.au

[1] School of Geography, Earth and Atmospheric Sciences, The University of Melbourne, Parkville, VIC 3010, Australia

[2] Geoscience Australia, GPO Box 378, Canberra, ACT 2601, Australia

[3] Zhejiang University, 866 Yuhangtang Rd, Xi Hu, Hang Zhou 310027, Zhe Jiang, China

the Meckering earthquake in 1968 and following global trends, seismic loading began to be included in the design of new dams. This became more formalized with the adoption of seismic hazard assessments (McCue 1995; ANCOLD 2003; 2019).

Australian dams are predominantly concrete gravity dams (e.g., the Burrinjuck Dam completed in 1928) and earthfill embankment dams, which are more common in rural areas and were constructed throughout the twentieth century. Many older dams have recently undergone structural upgrades to meet more stringent seismic design criteria. Australia's seismic design standards for dams are generally governed by the Australian National Committee on Large Dams (ANCOLD). ANCOLD provides guidelines for assessing the seismic performance of dams, which are aligned with international best practices. The seismic design criteria typically consider: Operating Basis Earthquake (OBE)—the maximum ground motion intensity at the dam site for which only minor and repairable damage is anticipated; and Maximum Credible Earthquake (MCE)—the largest conceivable earthquake magnitude or ground motion considered possible in a defined region (c.f., ANCOLD 2019). Australian dams have been categorized in terms of risk, consistent with practices in other countries. ANCOLD has established a risk framework that considers both the likelihood of dam failure and the potential consequences. Dams are categorized into different risk levels based on the potential consequences of failure, such as loss of life, environmental impact, and economic losses. "Extreme Consequence" and "High Consequence" refers to dams where failure could result in significant loss of life or environmental damage. These dams should be designed and maintained to the highest safety standards. "Low Consequence" means the failure of these dams is expected to have minimal impact, and their design standards are less stringent (ANCOLD 2019).

The 2019 ANCOLD Guidelines for Design of Dams and Appurtenant Structures for Earthquake outline the Requirements of a Seismic Hazard Assessment. They state, "*Information on any known active or neotectonic faults which have the capability to cause displacement in the foundation of the dam, appurtenant structures, or reservoir rim should be provided"* (ANCOLD 2019). An Active Fault is defined as "*A fault, reasonably identified and located, known to have produced historical earthquakes or showing evidence of movements in Holocene time (i.e. in the last 11,000 years) and large faults that have moved in Latest Pleistocene time (i.e. between 11,000 and 35,000 years ago)*" (ANCOLD 2019). A Neotectonic Fault is defined in the ANCOLD Guidelines as "*A fault, not active as defined above, that has experienced displacement under conditions imposed in the current crustal stress regime and hence may move again in the future*" (ANCOLD 2019). The primary source for the locations of Active and Neotectonic faults in Australia is the Australia Neotectonic Features Database (NFD) (https://neotectonics.ga.gov.au) that is hosted and maintained by Geoscience Australia. In the NFD, 'neotectonic features' are collectively defined as *'intraplate faults, fault-related folds, and other features that are demonstrated or suspected to relate to earthquakes large enough to deform the Earth's surface (i.e., mostly $M > 6$)* [and that] *are considered likely to have been the source of hazardous ground shaking during the period that the current crustal stress field has pertained (i.e., the past 6–10 million years), and so may pose a future hazard'*.

Categorizing faults as either '*active*' or '*neotectonic*' as recommended in the ANCOLD guidelines has specific implications for deterministic seismic hazard analysis for *Extreme Consequence Category* (*ECC*) dams. *ECC* dams are defined in ANCOLD (2012) as those with ≥ 100 population at risk and / or potential loss of life ≥ 5 in event of dam catastrophic damage and loss, and/or ≥ 1,000 population at risk and / or ≥ 50 potential loss of life in event of dam major damage and loss. In evaluating the recommended maximum level of ground motion for which a *ECC* dam should be designed or analysed (i.e., *Safety Evaluation Earthquake, SEE*) ANCOLD guidelines recommend the greater of the 85th percentile ground motion from the *MCE* on known *active faults* or the 85th percentile for the 1 in 10,000 annual exceedance probabilistic (*AEP*) ground motion derived from probabilistic seismic hazard analysis (PSHA). Ground motions should be computed and compared for the period range of most relevance to the dam and appurtenant structures (ANCOLD 2019). In terms of earthquake magnitude, ANCOLD defines the *MCE* as "*the largest reasonably conceivable earthquake magnitude that is considered to be possible along a recognized fault or within a geographically defined tectonic province, under the presently known or presumed tectonic framework*". In this study we use the term *maximum moment magnitude* ($M_{w,max}$; e.g., Clark et al. 2010) ground motion (i.e., $M_{w,max}$ *ground motion*) when describing fault-based ground motion model outputs because (i) it allows for discrimination between source-fault ground motions and *PSHA* ground motions and (ii) ground motions from comparatively smaller M_w events could exceed those from larger M_w events, even for earthquakes sourced from the same fault, due to a variety of source- and site-related aspects. PSHA-derived ground motions are referred to *NSHA23* ground motions in this study, because we use ground motion outputs from the 2023 Australian National Seismic Hazard Assessment (NSHA23; Allen et al. 2023).

$M_{w,max}$ ground motions may exceed *NSHA23* ground motions for time intervals and response spectra ranges typically relevant to dam operations and safety evaluations (i.e., ≥ 10^3 to 10^4 yrs; 0 to 1 s periods). It therefore may be important to understand the rupture characteristics of dam-proximal faults (e.g., taken as faults within 100 km of a dam in this study) to reduce uncertainty in $M_{w,max}$

estimates and better characterise M_w-frequency across time intervals of interest. Some dam owners and operators consider the rigorous study of dam-proximal faults as best-practise due diligence. It is pertinent to note that population growth and development may be increasing hazard exposure and risk for some dams.

Probabilistic fault displacement hazard (PFDHA) may be another important consideration in dam seismic hazard analysis. PFDHA endeavours to compute the mean annual rate of earthquakes from a specific fault source exceeding a specified principal ground surface displacement at a specified location (e.g., Moss and Ross 2011). The probability of occurrence of distributed secondary (distributed) ruptures (e.g., antithetical faults, flexural slip faults) at sites more distal from the principal fault trace (i.e., the location of localized shear displacements as evidenced through geospatial-geological studies) may be computed. Interested readers are turned to Nurminen et al. (2020), Sarmiento et al. (2021), Moss et al. (2022) and references therein for discussion of PFDHA.

In this study we attempt to survey the nation-wide exposure of ANCOLD-registered dams (Fig. 1) to specific aspects of shaking and ground surface rupture hazard using Geoscience Australia's Neotectonic Features Database (NFD). The goal of the study is to obtain first-order estimates of seismic hazard at a standardized scale useful for general reference and regional comparisons. To undertake a study at this scale we make numerous generalizations and assumptions that we describe herein. This study intended to inform but not replace site-specific PSHA and PFDHA approaches.

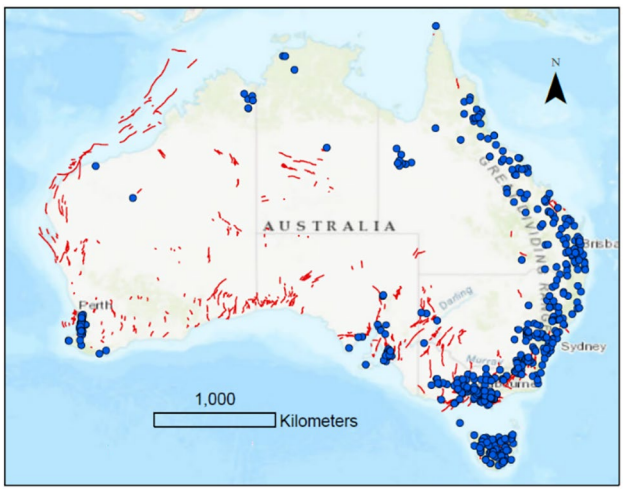

Fig. 1 NFD fault traces (red lines) and ANCOLD-registered dams (blue circles) considered in this study

2 Data and methods

2.1 Data

Geospatial data used in this study include:

(i) ANCOLD registry of large dams (https://ancold.org.au/wp-content/uploads/2023/04/Australia-2015-update-as-at-January-2022-with-disclaimer-1.xlsm
(ii) Geoscience Australia's Neotectonic Features Database (NFD) (https://www.ga.gov.au/applications/neotectonic-features-database)
(iii) Fault source model from NSHA23 (https://ecat.ga.gov.au/geonetwork/srv/api/records/76fef341-dcb8-42c7-9691-ff73ced58fd4)
(iv) NSHA23 (Allen et al. 2023)

2.2 Fault-dam distance calculations

We used ArcGIS Pro 2.4.0 software to identify NFD fault traces within a ≤ 100 km radius of ANCOLD dams (Fig. 1). This reduced the NFD faults considered to a population of 216 from 409. In 2011, the number of identified neotectonic faults was 230 (Clark et al. 2011). The approximate doubling of catalogued faults from 2011 to 2024 largely reflects continued fault mapping and analysis. NFD fault catalogue completeness is an important epistemic uncertainty in this study that can be reduced with ongoing mapping and analysis (Clark, 2023).

Using ArcGIS Pro "Near" functions we determined the nearest Euclidean distance point on the NFD fault trace to the central dam coordinates and visualised the line connections for each site (e.g., "R_5 *distance*" from Fig. 1 in Quigley et al. 2016; henceforth referred to in this paper as fault-dam distance). Two major uncertainties are acknowledged: (i) the relationship between dam central co-ordinates and actual spatial extent of dam infrastructure; and (ii) the relationship between NFD fault trace position and actual fault trace position (past and future). Depending on the area and orientation of dam infrastructure relative to the fault-dam distance, and the epistemic uncertainty related to fault position, we suggest these uncertainties could contribute a minimum of ± 250 m to the measured fault-dam distance. This is less important for larger (> 3–4 km) fault-dam distances but is highly relevant when considering whether a dam < 1 km from a fault trace could reside directly in the principal fault zone of a future earthquake. Detailed analyses of the spatial extents of dam infrastructure are beyond the scope of this study but could be used in future studies to reduce these uncertainties. An additional uncertainty is how the fault-dam distance relates to the distance from the dam to the fault at depth (subsurface distance, i.e., R_{rup}). Assuming a notional dip of 45 ± 15° (e.g., Sellmann et al.

2022) there may be instances where fault-dam distances are greater than, less than or approximately equal to R_{rup} and this could influence the ground motion modelling results. For most faults investigated here, limited information is available on their subsurface geometries; improving constraints on fault geometries near dam sites is identified as avenue for further research.

2.3 Fault characteristics: length, Mw, MD, AD, SR, RI

Data cleaning and spatial uncertainty corrections were applied to manage complex geometries of some NFD fault traces and to address database entries that contained length data variations due to the combinations of multiple fault sections into a singular entry. Surface fault trace lengths were obtained from the NFD database. Both parameters and their utility in subsequent calculations are subject to epistemic uncertainty and aleatory variability.

Earthquake scaling relationships appropriate for the Australian seismotectonic setting were used to estimate the M_w and single-earthquake displacements from fault lengths and areas (*Y21* = Yang et al. 2021; *Leo14* = Leonard 2014; *Som21* = Somerville 2021; *M22* = Moss et al. 2022). We assigned weightings based on consultation within the authorship team, noting that the weightings (i) differ from weights used in the NSHA23 analysis, and (ii) are uniformly used for all faults, noting that the NSHA23 varied weightings based on geological and seismo-tectonic setting.

- For M_w estimations, the length- M_w weightings are *Y21* = 0.1 and *Leo14* = 0.1 and area- M_w weightings are *Leo14* = 0.4 and *Som* = 0.4.
- For average displacement *(AD)*—M_w regressions the weightings are *Y21* = 0.34; *M22* = 0.33; *Leo14* = 0.33.
- For maximum displacement *(MD)*—M_w regressions the weightings are *Y21* = 0.5 and *M22* = 0.5.

Estimated fault slip rates (*SR*) were obtained from the *NSHA23* source model and used to estimate earthquake recurrence intervals (*RI*) assuming characteristic recurrence of $M_{w,max}$ earthquakes. For NFD faults with no listed *SR* we assumed a default *SR* of 10 m / Myr (the geometric mean of *NFD SR*). We used a fault inception age of 5 Ma (a minimum age for inception of the contemporary Australian intraplate stress field; Sandiford et al. 2004) and computed *AD* to calculate the *RI*.

- fault 'inception age' (i.e., the time interval over which cumulative fault displacements should be averaged to determine a slip rate; see Sellmann et al. 2022)
- fault kinematics and offsets (e.g., unless there is evidence to the contrary, all faults studied here are simplistically assumed to be reverse faults, based on high-angles between average fault trace strike and the average orientation of the maximum horizontal stress (see Rajabi et al., 2017) and studies of individual faults; displacement measurements, correlating offset features across the fault, etc.)
- slip-rate variability in time and space (e.g., episodicity; clustered rupture recurrence separated by long-term quiescence; how long-term slip rates relate to shorter term intervals and which is more appropriate to use in seismic hazard; see Clark et al. 2011)
- fault dip and geometry (see Mohammadi et al. 2019)
- fault rupture behaviour (e.g., segmentation vs. whole-fault rupture; possibility of multi-fault ruptures; see Quigley et al. 2016)
- the choice and weighting of scaling relationships (e.g., the Yang et al. 2021 regressions are derived from reverse faults in cratonic Australia alone; it is unclear how well this and the other regressions apply to faults with different kinematics and / or in non-cratonic Australia)

2.4 Modelled fault discrete and distributed displacements near dam sites

The primary fault displacements (i.e., the concentrated slip along a principal fault trace) at discrete locations on a fault (i.e., the *'discrete displacement"* = *D*), may be estimated relative to the anticipated *AD*, using the position of a discrete location along a fault trace (*x*) relative to the total length of the fault (*L*) (i.e., 'Normalized Position' in Fig. 2) (Moss and Ross 2011; Yang et al. 2021) (see also Fig. 2 caption). Dam-fault intersection lines are plotted on fault traces and this location is measured to most proximal fault trace termination. This distance is then converted into 'Normalized

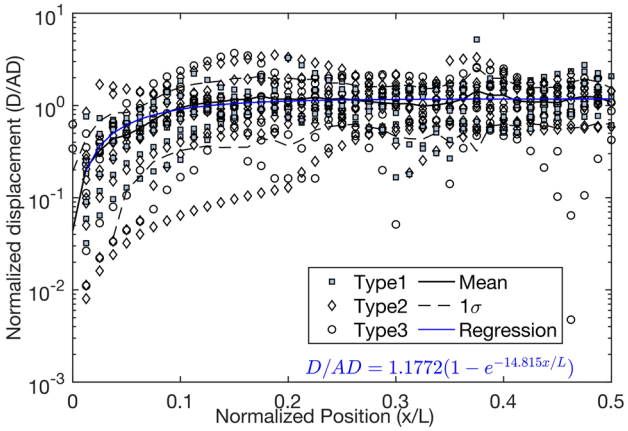

Fig. 2 Normalized displacement (D/AD) for Australian stable continental region earthquakes plotted as a function of rupture half length (x/L, where x/L = 0 is the rupture tip, and x/L = 0.5 is the rupture midpoint). SLR—surface rupture length. The regression equation is used to estimate D from AD at a given fault position

Position' by dividing by the fault length (Fig. 2). We assume fault displacement symmetry (noting this is an epistemic uncertainty) and thus a location in the central part of the fault = 0.5 and locations towards either end of the fault trend towards 0. A new Australia-based regression for estimating discrete displacement (D) at a fault position relative to AD is proposed in Fig. 2, based on the surface-rupture data presented in Yang et al. (2021). We note that all historic surface rupturing earthquakes have occurred cratonic central and western Australia, and therefore the utility of this regression to forecasting displacements in non-cratonic eastern Australia is an epistemic uncertainity. Between the 10th and 90th percentiles along the fault length (i.e., Normalized Position > 0.1 on Fig. 2), displacement at the dam-fault intersection line is ≥ AD. For the entire fault excluding the rupture tip, the incremental maximum displacement is estimated as ≈ MD. If the rupture tip is the closest location on the fault to the dam, average and maximum incremental displacements are ≈ 0. When considering primary fault-displacement-hazard analysis for a specific dam, we suggest fault traces that pass within ca. 500 m to 1 km of dams warrant detailed PFDHA investigation; 33 ANCOLD dams are found to meet the ≤ 1 km mean distance from dam criteria.

Reverse faulting distributed deformation regressions from Moss et al. (2022) were used to estimate the probability of a ground surface rupture feature within a 500 m^2 pixel centred on the dam centroid in the event of a $M_{w,max}$ earthquake on proximal NFD faults. Regressions were selected for use based on $M_{w,max}$ and on hanging wall or footwall positions of the dams relative to faults. The outputs of these regressions provide probabilities of at least one ground surface rupture occurrence at distances greater or equal to a specified distance. To compute the probability of rupture within the dam-hosting pixel, separate calculations were conducted for (mean-250 m) and (mean + 250 m) and differenced to obtain a discrete probability (this is distinct from the approaches in Moss et al. 2022 and Nurminen et al. 2022). There is substantive variation and aleatoric uncertainty in the outputs of the regressions. We plot discrete probability outputs vs. distance for different regressions from the fault displacement hazard initiative (FDHI) data (Moss et al. 2022) to provide users with first-order probability estimates. Ongoing developments in PFDHA regressions may reduce the epistemic uncertainty in appropriate regression selection. Appropriate weighting of the regressions could form part of ongoing work (as well as inclusion of other regressions). The work we present here is not intended to replace site specific PFDHA (including probability of distributed deformation) and should not be used as such.

We use the logistic regression for the occurrence of distributed rupture proposed in Visini et al. (2025) to estimate the probability of ground surface rupture of a distributed nature, using the same 500 m^2 pixel site dimension. This empirical regression is based on the latest SURE2.0 database (Nurminen et al. 2022). We calculate the probability based on $M_{w,max}$ and the hanging wall or footwall position of dams relative to faults, with the style of faulting (SoF) fixed as reverse. Following Nurminen et al. (2022), distributed ruptures (DRs) were classified into ranks based on local geological settings: Rank 1 (principal fault), Rank 1.5 (primary DR), Rank 2 (simple DR), Rank 2.1 (bending-moment), Rank 2.2 (flexural-slip), and Rank 3 (triggered faulting). To simplify the exploration of occurrence probabilities, three combination scenarios are proposed (Visini et al. 2025): Combination A (Rank 2 with respect to Rank 1 rupture traces), Combination B (Rank 2 with respect to Rank 1.5 rupture traces), and Combination C (Rank 1.5, 2.1, 2.2, or 3 with respect to Rank 1 rupture traces). We calculate probabilities for all combinations, and the overall probability is taken as the complement of the probability that none of the combinations occur, as we cannot yet exclude any possible combination.

To estimate ground motion intensities in the event of $M_{w,max}$ on dam proximal faults (i.e., deterministic approach), we used $M_{w,max}$ and dam-fault distances as inputs into the same set of GMMs (with the relative weights unchanged as well to avoid any additional uncertainties, see Table 1) that used in NSHA23 (Allen et al. 2023). To conduct a study of this scale we make many generalizations. As most dams can be considered more susceptible to short-period ground motions (e.g. Park and Kishida [2019]; Zimmaro and Ausilio [2020]), we selected the PGA and PSA[1.0 s] instead of other intensity measures for utilization in these analyses. We estimated the PGA and PSA[1.0 s] values under Cratonic and non-Cratonic conditions depending on the geological setting of the dam. For all dam sites we assume a general NEHRP B/C rock site (i.e., V_{S30} = 760 m/s). The GMM outputs are converted into 85th percentile intensities, as suggested in the ANCOLD guidelines for Extreme Consequence Dams. We acknowledge that a diversity of dam types, geometries and heights, designs, ages, site and foundation conditions

Table 1 GMMs and associated weights for Cratonic and Non-Cratonic conditions for deterministic ground motion calculations (Allen et al. 2023)

Model	Cratonic	Non-Cratonic	Reference
A12	0.24	0.29	Allen (2012)
AB06	0.13	0.15	Atkinson and Boore (2006)
D15	0.14	0.17	Drouet (2015)
ESHM	0.10	0	Weatherill et al. (2020)
NGAE	0.09	0.10	Goulet et al. (2017)
S09YC	0.16	0	Somerville et al. (2009)
S09NC	0.14	0.29	Somerville et al. (2009)

are present in the ANCOLD database; our results are not intended to replace site-specific, dam-specific analysis.

Probabilistic ground motions for dam locations were estimated using NSHA23(Allen et al. 2023). NSHA23 is calculated on a grid of sites, and PGA and PSA[1.0 s] hazard values with a 1/ 5,000 annual exceedance probability (AEP) from this grid were interpolated to dam locations. NSHA23 uses combinations of several ground motion models weighted in separate logic trees for cratonic and non-cratonic Australia. Maximum magnitudes on faults in NSHA23 were defined using a combination of structured expert judgement (varying for different neotectonic domains; Griffin et al. 2018; 2020) and area-based earthquake scaling relations (used in the case that fault dimensions were too small to host the $M_{w,max}$ determined by expert judgement; Leonard 2014). As recommended in ANCOLD 2019 for Extreme Consequence Dams, we use 85th percentile () NSHA23 PGA and PSA[1.0 s] values for comparison purposes. We compare deterministic intensities (PGA and PSA[1.0 s]) for $M_{w,max}$ from GMMs against probabilistic intensities for 1/5000 AEP from NSHA23 for different fault *RI* and *SR* parameters.

We calculate the fractional ratio of deterministic $M_{w,max}$ *intensity* values for GMMs to probabilistic NSHA23 *intensity* values and take $\log_{10}$ of this ratio for better illustration purpose. Positive values ($M_{w,max}$ *GMM intensity* > *NSHA23 intensity*) indicate scenarios where deterministic 85th percentile intensities for a given dam (i.e., proximal fault-based ground motion hazard) exceed the 1/5000 AEP derived from NSHA23 (i.e., 85th percentile probabilistic ground motion hazard including faults, seismicity). We only take the maximum positive value of $M_{w,max}$ intensity vs. NSHA23 intensity for each dam and plot the ratio (i.e. $M_{w,max}$ *GMM* intensity / NSHA23 intensity) considering other factors towards seismic hazard (e.g., slip rate and recurrence interval). Some aspects of our study favour the predominance of deterministic $M_{w,max}$ *GMM* intensity values over NSHA23 ones; for example: (i) using longer AEP intervals (e.g., 1:10,000 years) would increase NSHA23 intensity values and reduce *the radio*; (ii) using segmentation models for faults and assuming $M_{w,max} = 7.5 \pm 0.2$ (Clark et al. 2010) would decrease $M_{w,max}$ *GMM* intensity values and reduce the ratios;

3 Results

We identify 216 faults at 0 to 100 km distance from 428 dams and measure 4055 fault-to-dam distances (Fig. 3). At least 31 dams have a central location within 1 km of NFD fault traces. When accounting for positional and mapping uncertainties in dam-fault distances, at least 16 dams could reside within possible NFD primary fault zones (i.e., the lower bound of the ± 250 m uncertainty buffer applied to dam-fault distances is < 20 m from the currently mapped NFD fault trace). Detailed paleoseismic studies of these dam-proximal faults is recommended, particularly for Extreme and High Consequence Category dams.

We summarize key results of the ground displacement analysis as:

- Surface fault trace lengths for NFD faults used in this study range from 2 to 200 km (mean = 44 ± 31 km (1σ); median = 37 km).
- Preferred $M_{w,max}$ estimates from weighted averaging of area- and length-scaling relationships range from 5.6 to 7.9 (mean = 7.0 ± 0.4 (1σ); median = 7.1) (Fig. 3).
- Fault slip rates range from < 1 m / Myr to 990 m / Myr (mean = 35 m/Myr; median = 16 m / Myr) (Fig. 4a). Four faults have average slip rates ≥ 0.1 mm per year (Fig. 4b).
- *AD* ranges from < 0.3 m to 4.4 m (mean = 1.6 ± 0.8 m (1σ); median = 1.4 m) (Fig. 4b). 162 faults have AD ≥ 1.0 m (Fig. 4b).

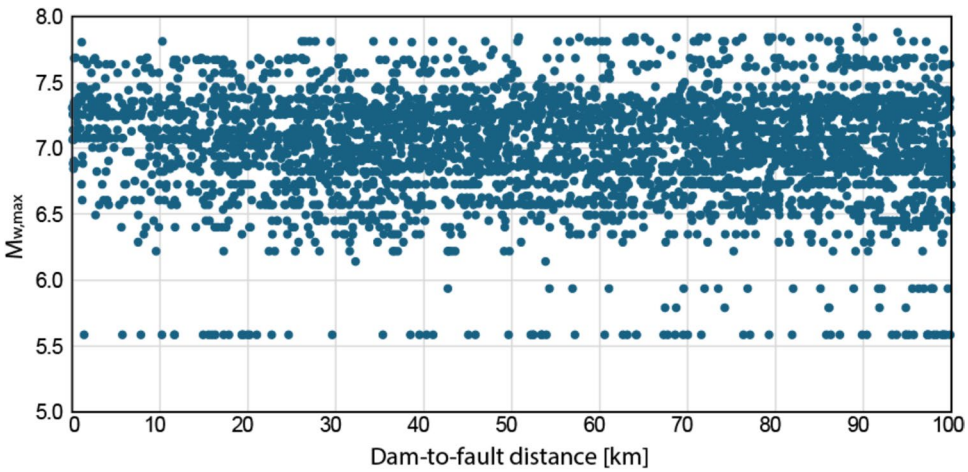

Fig. 3 Fault-to-dam distances vs. $M_{w,max}$

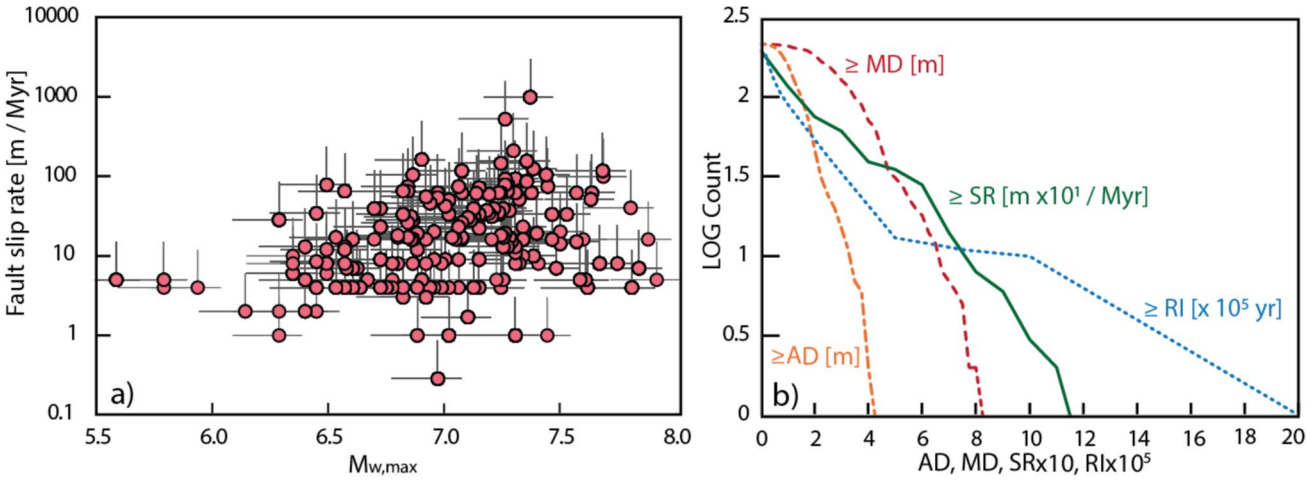

Fig. 4 **a** NFD fault slip rates vs. $M_{w,max}$. **b** Cumulative frequency of exceedance of AD, MD, SR and RI for NFD faults (n = 216)

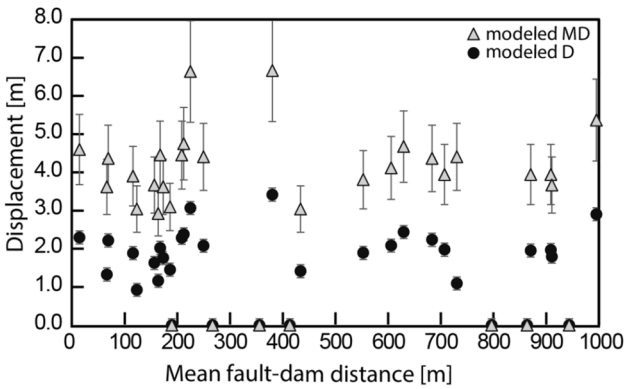

Fig. 5 Maximum fault displacements and discrete fault displacements (scaled from AD using the regression in Fig. 2) for $M_{w,max}$ scenarios on faults within 1 km of dam sites

- *MD* ranges from < 0.9 m to 8.4 m (mean = 3.7 ± 0.1 m (1σ); median = 3.5 m) (Fig. 4b).
- $M_{w,max}$ RI ranges from ca. 24 kyr to > 2 Myr with a mean RI of ca. 200 kyr (median = ca. 85 kyr). The concept of periodic 'recurrence intervals' of characteristic $M_{w,max}$ events is a major assumption that may not accurately represent rupture behaviours on many NFD faults.
- Substantial fault-specific research is required to evaluate the credibility of these estimates, with the largest estimates exceeding values typically assumed for continental Australia (e.g., Griffin et al. 2018).

Of the 33 faults within 1 km of dam sites, 25 have modelled discrete displacements > 1 m and modelled *MD* > 3 m (Fig. 5). In all 33 cases, increasing the accuracy and precision of NFD fault trace locations relative to dam infrastructure may be advantageous, because dam sites most proximal to the ends of a fault trace return modelled displacement values of 0 that do not reflect the epistemic uncertainty that future primary ground surface ruptures could extend beyond the mapped NFD traces.

At fault-dam distances < 1000 m, discrete probabilities of distributed rupture in the 500 × 500 m pixel centred on the dam centroid in event of $M_{w,max}$ earthquakes range from ca. 0.1 to > 0.5 for dams in fault footwalls and > 0.1 to > 0.5 for dams in fault hanging walls. Depending on which regression is used, as many as 40 dams have a ≥ 10% probability of ground surface rupture occurring in the area encompassing the dam in a $M_{w,max}$ event. Further development of distributed fault displacement hazard analyses and regressions, including development of functions for Australian conditions, is a prospective avenue for further research. The new regressions (based on FDHI functions) in Fig. 6 provide first-order approximations, are limited only to the fault-to-site distance ranges shown in the figures and are subject to large and currently uncharacterised epistemic and aleatoric uncertainties that may limit their direct utility in PFDHA.

Figure 7 shows that, generally, the hanging wall exhibits a higher probability of distributed ruptures (DRs) for all combinations. For both footwall and hanging wall faulting, Combination A contributes most to the overall DR probability, assuming no information is available to discount the assumptions of Combinations B and C. Furthermore, Figs. 6 and 7 show that the probability of distributed faulting from the FDHI database (Moss et al. 2022) is similar to that of Combination A from the SURE2.0 database (Visini et al. 2025), while the probability of distributed and complex faulting from the FDHI database is similar to that of Combination C from the SURE2.0 database. These interesting results suggest that the two databases can provide comparable estimates of conditional distributed surface ruptures, with similar levels of uncertainty. Real-case applications may employ a logic-tree approach to address the epistemic

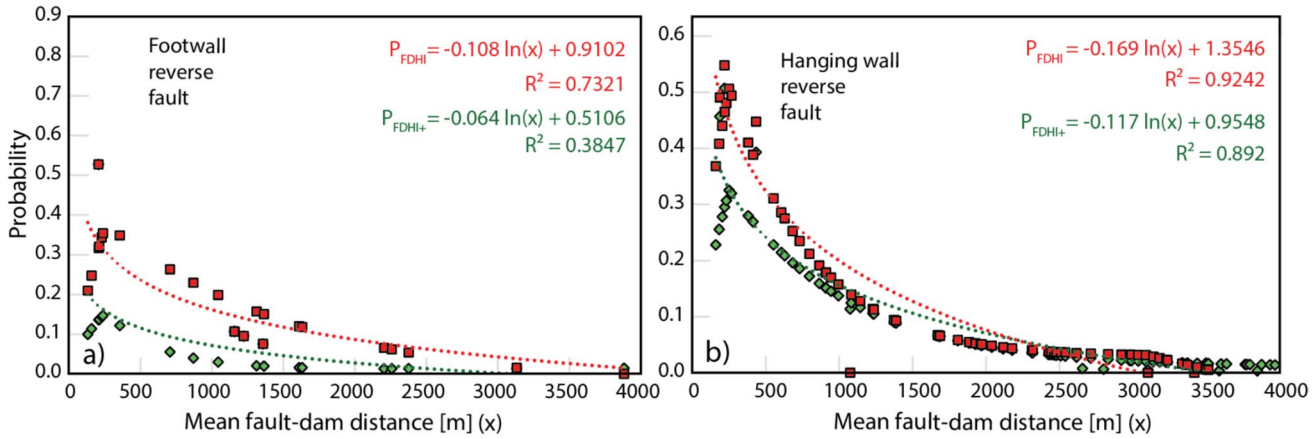

Fig. 6 **a**: Discrete probability of ground surface rupture within a 500 × 500 m pixel centred on the dam centroid using two regressions: (i) P_{FDHI} (distributed faulting; Moss et al. 2022); (ii) P_{FDHI+}(distributed faulting + complex faulting conditions; Moss et al. 2022). Moss et al. 2022 define 'Complex faulting conditions' as 'complex fault systems where distributed displacements may occur at distance due to sympathetic release on adjacent or nearby faults'. Regressions provide only crude estimates of at least one rupture occurring within the pixel with a centre distance (mean fault-dam distance) from the mapped NFD trace; further refinement of the regressions may reduce epistemic uncertainty in their application

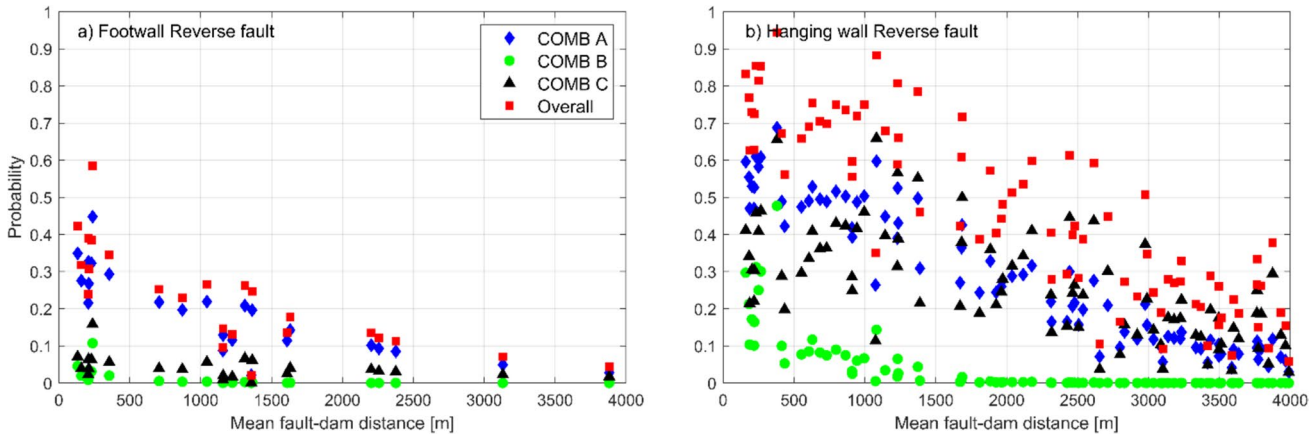

Fig. 7 **a**: Probability of distributed surface rupture with a 500 × 500 m site dimension using three combinations (Visini et al. 2025): (i) COMB A: Rank 2 with respect to rupture traces of Rank 1; (ii) COMB B: Rank 2 with respect to rupture traces of Rank 1.5; and (iii) COMB C: Rank 1.5, 21, 22, or 3 with respect to rupture traces of Rank 1. The displacement ranking is adopted from Nurminen et al. (2022): Rank 1 refers to principal fault), Rank 1.5 for primary DR, Rank 2 for simple DR, Rank 21 for bending-moment DR, Rank 22 for flexural-slip DR and Rank 3 for triggered faulting DR

uncertainties associated with different models (Visini et al. 2025).

3.1 Ground motion exceedance

Key aspects of the ground motion analysis include:

- For the 4055 considered scenarios, approximately 88% (n = 3579) yield 85th percentile deterministic $M_{w,max}$ PGA estimates ≥ 0.1 g, and the number for PSA[1.0 s] is 70% (n = 2844).
- For the 428 scenarios for dams with maximum ground motion intensities, approximately 94% (n = 402) yield 85th percentile deterministic $M_{w,max}$ PGA that exceed the 85th percentile NSHA23 PGA with 1/5000 AEP, and the number for PSA[1.0 s] is 99% (n = 422).
- There are 341 instances (11 faults) where $M_{w,max}$ *PGA* are ≥ 0.1 g and fault slip rates are ≥ 100 m / Myr (i.e., 0.1 mm/yr), and the number for $M_{w,max}$ PSA[1.0 g] is 299 (11 faults). These faults could be prioritised for further research.
- There are 29 dams (6.5%) where:

- the mean deterministic *PGA* for $M_{w,max}$ for the earthquake scenario that generates the largest *PGA* is ≥ 0.1 g, and
- the *PGA* for this $M_{w,max}$ *PGA* is greater than the corresponding NSHA23 1/5,000 AEP *PGA*, and
- the fault that contributes to this hazard has a slip rate ≥ 100 m / Myr (Fig. 8).
- There are 32 dams (7.5% of 428 dams) where:
- the mean deterministic *PSA[1.0 s]* for $M_{w,max}$ for the earthquake scenario that generates the largest *PSA[1.0 s]* is ≥ 0.1 g, and
- the *PSA[1.0 s]* for this $M_{w,max}$ *PSA[1.0 s]* is greater than the corresponding NSHA23 1/5,000 AEP *PSA[1.0 s]*, and

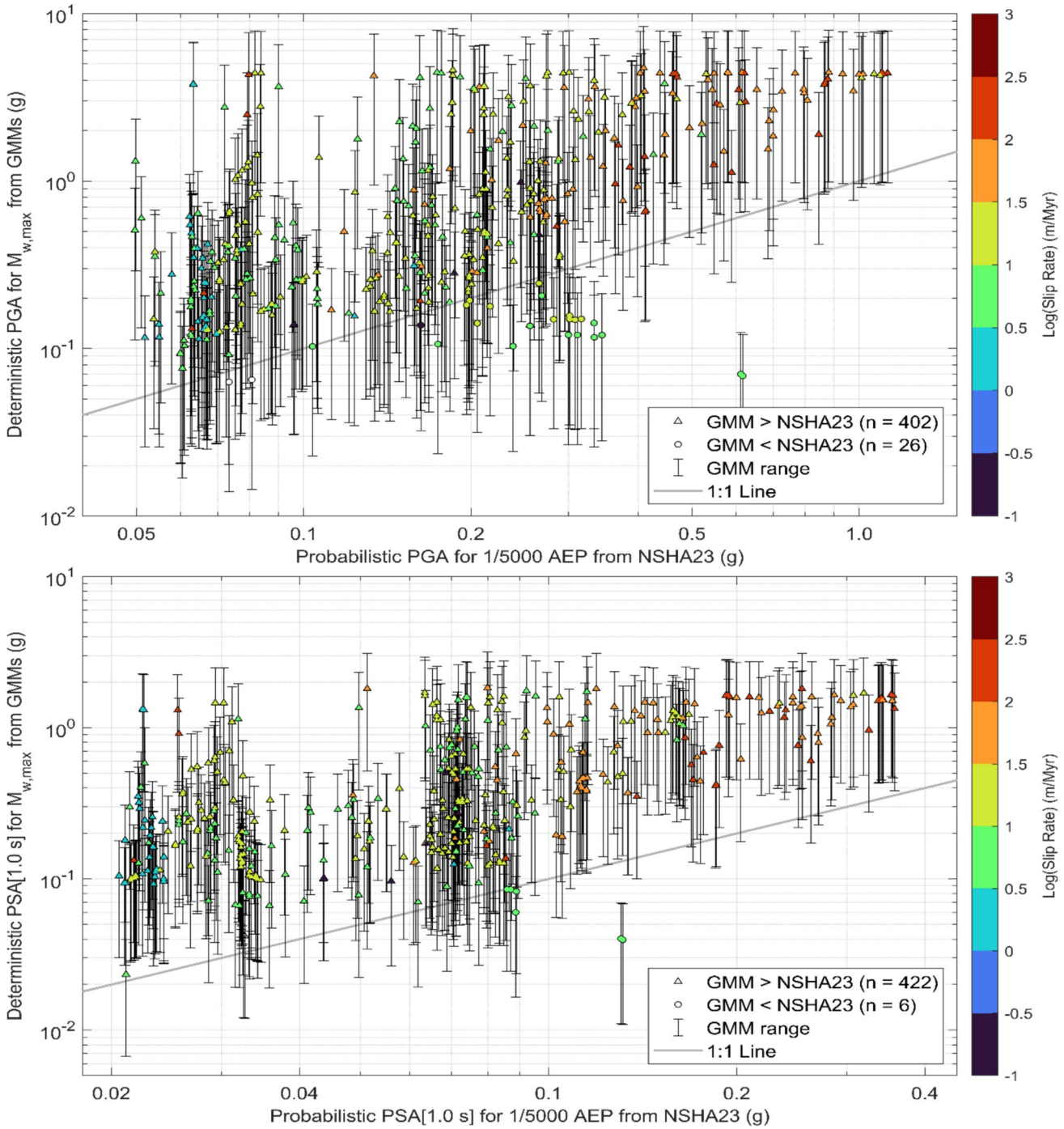

Fig. 8 GMM intensity vs NSHA23 intensity coded for slip rate **a** $M_{w,max}$ PGA, **b** PSA[1.0]

- the fault that contributes to this hazard has a slip rate ≥ 100 m / Myr (Fig. 8).

There are 241 dams with the same criteria but lowering the slip rate to ≥ 10 m / Myr for *PGA* (Fig. 8) and 285 for *PSA[1.0 s]*. Given the potential for large (perhaps even exceeding an order of magnitude) temporal variations and associated uncertainty in slip rates for some faults (e.g., Clark et al., 2015), rigorous studies of proximal faults could be considered as part of due diligence seismic hazard analysis for these dams.

Map plots of the (log10) ratio of the largest 85th percentile deterministic $M_{w,max}$ *intensities* for each dam vs. the corresponding NSHA23 *intensities* show large spatial and magnitude variations in the relative contributions of fault-based vs. PSHA-based hazard levels (Figs. 9 and 10). There is a tendency for *GMM* $M_{w,max}$ *PGA and PSA[1.0 s]* hazard levels to dominate for fault-proximate (i.e., within 0 to 30 km) dam locations, particularly for larger faults, and in areas of lower seismicity. NSHA23 *PGA* and *PSA[1.0 s]* hazard levels tend approach or exceed *GMM* $M_{w,max}$ *PGA* and *PSA[1.0 s]* hazard levels more distal from NFD faults, and in areas of higher seismicity. Consideration could be given to enhancing knowledge of NFD faults in areas where the *GMM* $M_{w,max}$ *PGA* and *PSA[1.0 s]* hazard levels are well in excess of *NSHA23*ones. For most (approx. 90–95%) NFD faults, the timing and characteristics of pre-instrumental earthquakes with sufficient M_w to generate ground surface rupture and produce strong, potentially damaging ground motions have not been directly established through detailed geologic-geomorphic-chronologic studies.

4 Conclusions

A geospatial and statistical approach is used to characterise the exposure of ANCOLD-registered dams to faults in the Australian Neotectonic Features Database. There are 216 NFD fault traces within 100 km of 428 ANCOLD dams. Allowing for geospatial measurement and mapping uncertainties, between 16 and 31 dams could be directly exposed to primary ground surface rupture hazard on NFD

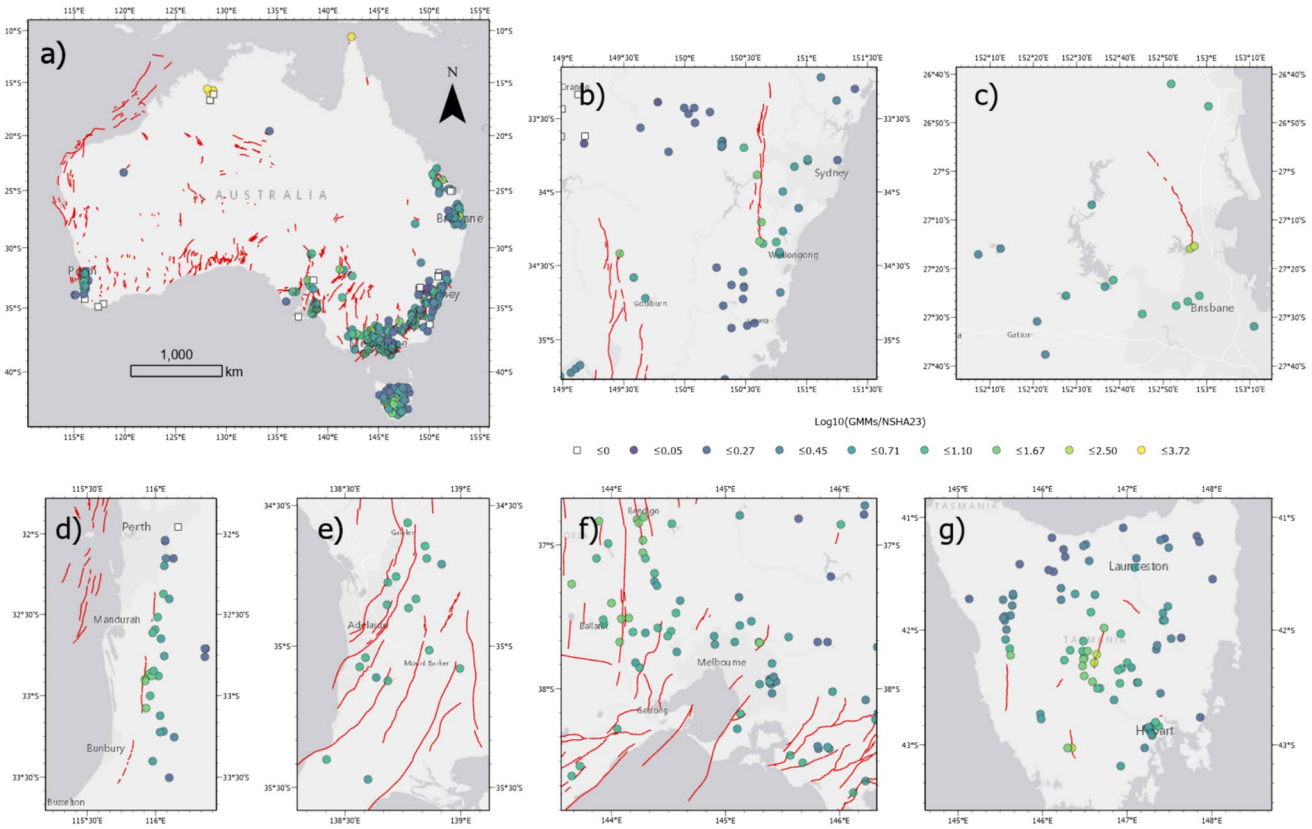

Fig. 9 **a** Log10 ratios of GMM PGA (g) vs NSHA23 1 in 5000 AEP PGA (g); **b** GMM PGA vs NSHA 23 1 in 5,000 AEP PGA for the Canberra and Sydney (ACT and NSW) region; **c** GMM PGA vs NSHA 23 1 in 5000 AEP PGA for the Brisbane (QL) region; **d** GMM PGA vs NSHA 23 1 in 5000 AEP PGA for the Perth (WA) region; **e** GMM PGA vs NSHA 23 1 in 5000 AEP PGA for the Adelaide (SA) region; **f** GMM PGA vs NSHA 23 1 in 5000 AEP PGA for the Melbourne (VIC) region; **g** GMM PGA vs NSHA 23 1 in 5000 AEP PGA for Tasmania region

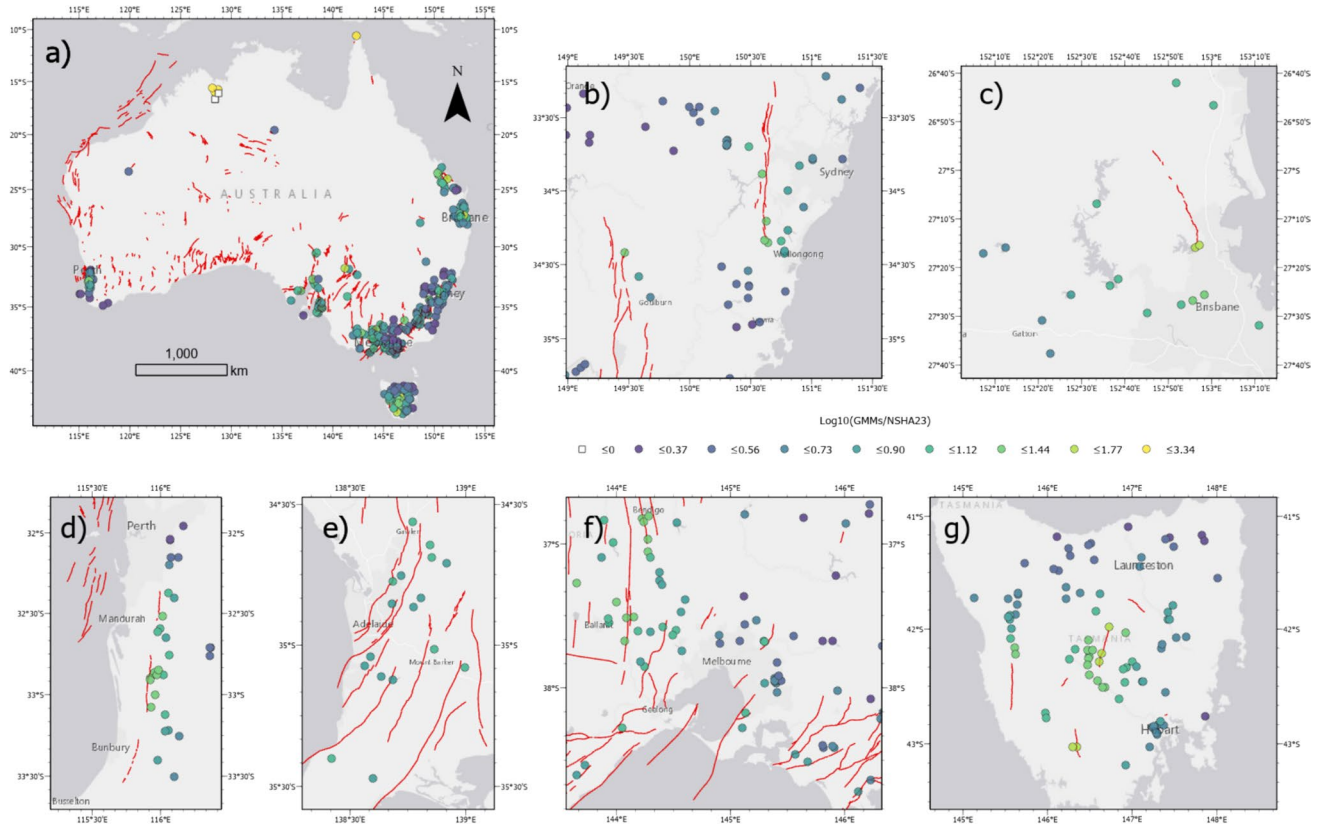

Fig. 10 **a** Log10 ratios of GMM PSA[1.0 s] (g) vs NSHA23 1 in 5000 AEP PSA[1.0 s] (g); **b** GMM PSA[1.0 s] vs NSHA 23 1 in 5000 AEP PSA[1.0 s] for the Canberra and Sydney (ACT and NSW) region; **c** GMM PSA[1.0 s] vs NSHA 23 1 in 5000 AEP PSA[1.0 s] for the Brisbane (QL) region; **d** GMM PSA[1.0 s] vs NSHA 23 1 in 5000 AEP PSA[1.0 s] for the Perth (WA) region; **e** GMM PSA[1.0 s] vs NSHA 23 1 in 5000 AEP PSA[1.0 s] for the Adelaide (SA) region; **f** GMM PSA[1.0 s] vs NSHA 23 1 in 5000 AEP PSA[1.0 s] for the Melbourne (VIC) region; **g** GMM PSA[1.0 s] vs NSHA 23 1 in 5000 AEP PSA[1.0 s] for Tasmania region

faults. Displacement modelling for $M_{w,max}$ earthquakes on most of these dam-proximal faults yields average displacements > 1 m and maximum displacements > 3 m. Many of these displacements exceed suggested tolerable limits for fault displacement through foundations (Wieland et al., 2008). As many as 40 dams have a ≥ 10% probability of ground surface rupture occurring in the area encompassing the dam in a $M_{w,max}$ earthquake based on the empirical regressions from the FDHI database (Moss et al. 2022). Detailed fault studies will increase knowledge of many dam-proximal faults to better support dam hazard and risk analyses. Fault studies could include mapping of fault traces with LiDAR and other high-resolution geospatial datasets, paleoseismic trenching to establish rupture characteristics from past earthquakes, geological and geophysical studies to better characterise fault geometries and displacements, and PFDHA.

Using a simplified modelling approach, deterministic *PSA* estimates for $M_{w,max}$ scenarios on NFD faults are derived from different ground motion models commonly used in Australia at a response spectral period relevant to dams (PGA and 1 sec. period). These results are compared to 1:5000 AEP *PGA* and *PSA* [1.0 s] derived from the NSHA23 (in terms of 85th percentile intensity). For the 4055 considered fault-dam combinations, approximately 88% (n = 3579) yield 85th percentile deterministic $M_{w,max}$ *PGA* estimates ≥ 0.1 g, and the number for *PSA* [1.0 s] is 70% (n = 2844).(in excess of typical thresholds for liquefaction triggering, e.g., Quigley et al. 2016). Although this comparison uses different values from the approach described for Extreme Consequence Dams in the ANCOLD guidelines, it provides a useful framework for evaluating relative hazard contributions. Detailed analyses of fault-based hazard may be particularly relevant for dams within 20–30 km of faults with sufficient length (e.g., ≥ 20–30 km) to produce Mw ≥ 6.7–> 7.0 earthquakes and sufficiently high slip rates (e.g., ≥ 0.1 mm yr^{-1}) to potentially contribute to time-dependent seismic hazard at time-scales commonly of interest for critical infrastructure (e.g., ≥ 5000–10,000 yr). Future work could include site specific PSHA for individual dams to establish mean PGA and PSA [1.0 s] at 1:10,000 AEP as per ANCOLD guidelines. Preliminary investigations

suggest ratios of 1:10,000 to 1:5,000 AEP for these parameters are approximately 1.5.

Acknowledgements The authors thank Trevor Allen for seismic analyses and participation in scientific discussions. The authors thank Jack Williams (Otago) and two anonymous reviewers for reviewing this manuscript.

Author contribution M.Q. wrote the main manuscript text with contributions from T.W. & G.T. Geospatial analyses conducted by T.W. & M.Q. Fault analyses conducted by M.Q., D.C. G.T. & H.Y. Seismological analyses performed by G.T., J.G. & M.Q. Figures prepared by M.Q., T.W., & G.T. All authors reviewed and provided revisions to the manuscript.

Funding Open Access funding enabled and organized by CAUL and its Member Institutions. NEMA Disaster Ready Fund, DRF40204, DRF40204, DRF40204, DRF40204, DRF40204

Data availability Readers interested in obtaining dam-specific data should contact M.Q. via email. The datasets developed and analysed in this study are available for download at: https://github.com/Y-Tang99/Online-Data/blob/main/Quigley_et_al_ESD_2025_Supplementary_Document.zip.

Declarations

Conflict of interest The authors declare no conflict of interests.

References

Allen, T. I., Griffin, J. D., Clark, D. J., Cummins, P. R., Ghasemi, H., & Ebrahimi, R. (2023). The 2023 National Seismic Hazard Assessment for Australia. *Geoscience Australia Record 2023/53*.

Allen, T. I. (2012). Stochastic Ground-motion Prediction Equations for Southeastern Australian Earthquakes using Updated Source and Attenuation Parameters, Geoscience Australia, Canberra, Record 2012/69.

ANCOLD (2003). Guidelines on the Consequence Categories for Dams. ANCOLD, Australia, pp 15–30.

ANCOLD (2012). Guidelines on the Consequence Categories for Dams (2012).

ANCOLD (2019). ANCOLD guidelines for design of dams and appurtenant structures for earthquake. July 2029.

Atkinson GM, Boore DM (2006) Earthquake ground-motion prediction equations for eastern North America. Bull Seismol Soc Am 96:2181–2205. https://doi.org/10.1785/0120050245

Clark DJ (2023) The 2023 National Seismic Hazard Assessment for Australia: notes on fault fault parametrisation for the fault-source model. Geoscience Australia Record 2023/54, pp 47. https://doi.org/10.26186/149143

Clark et al. 2011 Australia's seismogenic neotectonic record

Clark D, McPherson A, Collins C (2010) Mmax estimates for the Australian stable continental region (SCR) derived from palaeoseismicity data. Australian Earthquake Engineering Society 2010 Conference, Perth, Western Australia, p 15

Clark D, McPherson A, Collins CDN (2011) Australia's seismogenic neotectonic record: a case for heterogeneous intraplate deformation. Geoscience Australia Record 2011/11, Canberra, p 95.

Clark D, McPherson A, Cupper M, Collins C, Nelson G (2015) The Cadell Fault: a record of temporally clustered morphogenic seismicity in a low-strain intraplate region, south-eastern Australia. In: Seismicity, fault rupture and earthquake hazards in slowly deforming regions, vol. 432. Geological Society of London Special Publication

Drouet, S. (2015). drouet_2015_brazil.py, Global Earthquake Model oq-engine. Retrieved 24 January, 2024, from https://github.com/gem/oq-engine/blob/master/openquake/hazardlib/gsim/drouet_2015_brazil.py.

Goulet, C. A., Y. Bozorgnia, N. Kuehn, L. Al Atik, R. R. Youngs, R. W. Graves, and G. M. Atkinson (2017). NGA-East ground-motion models for the U.S. Geological Survey National Seismic Hazard Maps, Pacific Earthquake Engineering Research Center PEER Report No. 2017/03, pp 180.

Griffin JD, Allen TI, Gerstenberger MC (2020) Seismic hazard assessment in Australia: can structured expert elicitation achieve consensus in the "land of the fair go"? Seismol Res Lett 91(2A):859–873

Griffin, J., Gerstenberger, M., Allen, T. and Venkatesan, S., 2018. Expert elicitation of model parameters for the 2018 National Seismic Hazard Assessment: Summary of workshop, methodology and outcomes. *Geoscience Australia Record 2018/28*.

Leonard M (2014) Self-consistent earthquake fault-scaling relations: update and extension to stable continental strike-slip faults. Bull Seism Soc Am 104:2953–2965

McCue, K. F. (1995). Australian Seismicity: A Review, Australian Earthquake Engineering Society (AEES), pp 10–45.

Mohammadi H, Quigley M, Steacy S, Duffy B (2019) Effects of source model variations on Coulomb stress analyses of a multi-fault intraplate earthquake sequence. Tectonophysics 766:151–166

Moss, R., Thompson, S., Kuo, C.H., Younesi, K. and Baumont D. (2022). Reverse Fault PFDHA, University of California, Los Angeles, Report GIRS-2022–05, https://doi.org/10.34948/N3F595.

Moss RES, Ross ZE (2011) Probabilistic fault displacement hazard analysis for reverse faults. Bull Seismol Soc Am 101(4):1542–1553

Nurminen F, Boncio P, Visini F, Pace B, Valentini A, Baize S, Scotti O (2020) Probability of occurrence and displacement regression of distributed surface rupturing for reverse earthquakes. Front Earth Sci 8:581605

Nurminen F, Baize S, Boncio P, Blumetti AM, Cinti FR, Civico R, Guerrieri L (2022) SURE 2.0—New release of the worldwide database of surface ruptures for fault displacement hazard analyses. Sci Data 9(1):729

Park DS, Kishida T (2019) Seismic response of embankment dams based on recorded strong motion data in Japan. Earthq Spectra 35(2):955

Quigley M, Hughes M, Bradley B, van Ballegooy S, Reid C, Morgenroth J, Horton T, Duffy B, Pettinga J (2016) The 2010–2011 Canterbury earthquake sequence: environmental effects, seismic triggering thresholds, and geologic legacy. Tectonophysics. https://doi.org/10.1016/j.tecto.2016.01.044

Rajabi M, Tingay M, Heidbach O, Hillis R, Reynolds S (2017) The present-day stress field of Australia. Earth Sci Rev 168:165–189

Sandiford M, Wallace M, Coblentz D (2004) Origin of the in situ stress field in south-eastern Australia. Basin Res 16(3):325–338

Sarmiento A, Madugo D, Bozorgnia Y, Shen A, Mazzoni S, Lavrentiadis G, Dawson T, Madugo C, Kottke A, Thompson S, Baize S, Milliner C, Nurminen F, Boncio P, Visini F (2021) Fault displacement hazard initiative database. Report No. GIRS-2021-08, Revision 3.3. The B. John Garrick Institute for the Risk Sciences at UCLA Engineering, Los Angeles CA

Sellmann S, Quigley M, Duffy B, Yang H, Clark D (2022) Fault geometry and slip rates from the Nullarbor and Roe Plains of south-central Australia: Insights into the spatial and temporal characteristics of intraplate seismicity, Earth Surf. Process Landforms 48:350–370

Somerville P (2021) Scaling relations between seismic moment and rupture area of earthquakes in stable continental regions. Earthquake Spectra 37:1534–1549

Somerville, P., R. Graves, N. Collins, S. G. Song, S. Ni, and P. Cummins (2009). Source and ground motion models for Australian earthquakes, Australian Earthquake Engineering Society 2014 Conference, Newcastle, Australia, 11–13

Visini F, Boncio P, Valentini A et al (2025) Empirical regressions for distributed faulting of dip-slip earthquakes. Earthquake Spectra. https://doi.org/10.1177/87552930241308860

Weatherill G, Kotha SR, Cotton F (2020) A regionally-adaptable "scaled backbone" ground motion logic tree for shallow seismicity in Europe: application to the 2020 European seismic hazard model. Bull Earthq Eng. https://doi.org/10.1007/s10518-020-00899-9

Wieland, M., Bozovic, A., Brenner, A.P. (2008) Dam design – the effects of active faults. Water Power.

Yang H, Quigley M, King T (2021) Surface slip distributions and geometric complexity of intraplate reverse-faulting earthquakes. GSA Bull 133(9–10):1909–1929

Zimmaro F, Ausilio E (2020) Numerical evaluation of natural periods and mode shapes of earth dams for probabilistic seismic hazard analysis applications. Geosciences 10(499):1–11